Chinese Journal of
POLYMER SCIENCE

ARTICLE

https://doi.org/10.1007/s10118-018-2137-4
Chinese J. Polym. Sci. 2018, 36, 1027–1035

Synthesis of Poly(isosorbide carbonate) *via* Melt Polycondensation Catalyzed by Ca/SBA-15 Solid Base

Xiao-Long Shen[a,b], Zi-Qing Wang[a,c], Qing-Yin Wang[a], Shao-Ying Liu[a], and Gong-Ying Wang[a,c*]

[a] *Chengdu Institute of Organic Chemistry, Chinese Academy of Sciences, Chengdu 610041, China*
[b] *University of Chinese Academy of Sciences, Beijing 100049, China*
[c] *Changzhou Institute of Chemistry, Changzhou 213164, China*

Electronic Supplementary Information

Abstract Ca/SBA-15 solid bases with different Ca/Si atomic ratios were prepared by a one-pot route and employed as catalysts for the production of poly(isosorbide carbonate) (PIC) from diphenyl carbonate and isosorbide *via* a transesterification polymerization process. The relationship between physicochemical properties and catalytic performance for Ca/SBA-15 in this melt process was investigated by means of various characterization techniques. It was found that basic site amount and strength were responsible for this transesterification process; the weak and medium basic sites inclined to promote polycondensation reaction. It was worth noting that strong basic sites could favor the decomposition of the resultant PIC, resulting in the decrease of weight-average molecular weight (M_w) and yield, and the sample with Ca/Si atomic ratio of 0.4 exhibited the best catalytic performance, giving PIC with M_w of 4.88 × 10^4 g/mol and T_g of 169 °C at the optimal conditions. This excellent activity can be ascribed to the presence of rich basic sites and specific basic strength on the surface of 0.4Ca/SBA-15.

Keywords Ca/SBA-15; Poly(isosorbide carbonate); Diphenyl carbonate; Transesterification; Basic sites

Citation: Shen, X. L.; Wang, Z. Q.; Wang, Q. Y.; Liu, S. Y.; Wang, G. Y. Synthesis of Poly(isosorbide carbonate) *via* Melt Polycondensation Catalyzed by Ca/SBA-15 Solid Base. Chinese J. Polym. Sci. 2018, 36(9), 1027–1035.

INTRODUCTION

Polycarbonate (PC) as an outstanding engineering plastic, especially bisphenol A PC (BPA-PC), has been industrially applied in various fields due to its excellent properties, such as high tensile strength, impact resistance, durability and heat resistance[1–3]. However, bisphenol A (BPA), as a basic petroleum-based raw material for BPA-PC, is toxic, which leads to chronic toxicity and environment problems[4, 5]. Of the typical renewable monomers[6–10], isosorbide (1,4:3,6-dianhydro-D-glucidol, ISB) is an excellent candidate to replace BPA, owing to its attractive features, including rigidity, chirality and low toxicity[11, 12]. To date, ISB has been widely employed as a functional monomer to synthesize or modify polymers, such as polyesters[13, 14], polyamides[15, 16], polycarbonates[17–23] and other functional polymeric materials[24–26].

The synthesis of poly(isosorbide carbonate) (PIC) *via* the interfacial polycondensation of ISB with diphosgene or triphosgene and the melt polycondensation of ISB with dimethyl carbonate (DMC) or diphenyl carbonate (DPC) has been investigated. Although the former has successfully synthesized PIC, it is not economical or eco-friendly on account of the complicated processes and high toxicity reagent. Recently, melt polycondensation has drawn more attention for the advantages of low equipment requirements and non-toxic byproducts, in which the effective catalyst is the critical factor for the synthesis of PIC with satisfactory molecular weight. Using lithium acetylacetonate as a catalyst, Li *et al.*[21] prepared a PIC with M_w of as high as 4.65 × 10^4 g/mol by melt polycondensation of DMC with ISB. Cesium carbonate was also found to be a desirable catalyst for the polycondensation of DPC with ISB to obtain high-molecular-weight PIC[22]. However, homogeneous base would have negative effects on the application performance of the resultant polymer, such as exterior colours, toxicology and thermal stability[21, 22]. Most recently, Zhang *et al.*[23] designed a series of novel quaternary ammonium ionic liquids for the synthesis of PIC, and they found that tetraethylammonium imidazolate (TEAI) exhibited the highest catalytic activity, producing PIC with M_w of 2.56 × 10^4 g/mol. Unfortunately, although some basic ionic liquids were easily removed, the low catalytic activity resulted in a PIC with low molecular weight.

SBA-15 based solid bases as typical heterogeneous basic catalysts have been widely studied in the field of transesterification reactions for their ordered pore structure, thick pore walls, large pore size and high hydrothermal/

* Corresponding author: E-mail wanggongying1102@126.com
Received December 5, 2017; Accepted March 26, 2018; Published online April 25, 2018

thermal stability[27, 28]. Up to now, both organic and inorganic basic species, including amino[29], potassium[30], and calcium[31–33], have been introduced to SBA-15. Among them, calcium is the most popular one to modify SBA-15 owing to its good preservation of mesostructure, excellent water resistance and high specific surface area (S_{BET})[32, 33]. Nowadays, Ca/SBA-15 has been synthesized by a traditional impregnation method and one-pot route method. Using the former method to prepare Ca/SBA-15, strong/super bases can be generated in mesoporous silica. However, complex process of synthesis and strict storage conditions limit its industrial applications. On the other hand, one-pot route method has attracted more attention for its simpler synthesis process, better calcium species distribution, higher S_{BET} and stronger chemical stability[34]. Lou *et al.*[35] prepared Ca/SBA-15 by one-pot route for transesterification of vegetable oil with methanol, and the results showed that the higher catalytic activity was mainly related to its larger medium basic strength and higher S_{BET}. Additionally, inorganic calcium materials are also excellent fillers for polymers, which not only boost their mechanical properties but also can afford them new application performance[36]. Nevertheless, there are few publications on the use of Ca/SBA-15 as heterogeneous catalysts for polymer synthesis *via* the melt transesterification process.

In this work, the Ca/SBA-15 samples were also prepared by the so-called one-pot route and firstly used as catalyst for the transesterification of DPC with diols, and structure-activity relationship was discussed through gel permeation chromatography (GPC), differential scanning calorimetry (DSC), X-ray diffraction (XRD), Fourier transform infrared spectroscopy (FTIR), transmission electron microscopy (TEM), N_2 adsorption, thermogravimetric analysis (TGA), and CO_2 temperature-programmed desorption (CO_2-TPD).

EXPERIMENTAL

Materials and Reagents

Isosorbide (98%) purchased from Shanghai Yuanye Bio-Technology Co., Ltd was purified by recrystallization in absolute acetone. Commercial DPC purchased from Guangdong Guanghua Scitech Co., Ltd was purified by recrystallization in absolute ethyl alcohol. 1,3-Propanediol (98%) and 1,6-hexanediol (98%) were purchased from Shanghai Aladdin Bio-chem Technology. 1,4-Butanediol (99%), 1,5-pentanediol (98%), tetraethyl orthosilicate (TEOS) and $Ca(NO_3)_2{\cdot}4H_2O$ were supplied by Chengdu Kelong Chemical Reagent Co., Ltd.

Preparation of Catalysts

Ca/SBA-15 samples were prepared by a one-pot route according to literature[35]. Pluronic P123 (4 g) was dissolved in 150 g of 1.6 mol/L HCl with stirring at 40 °C for 0.5 h, and then a calculated amount of $Ca(NO_3)_2$ was added until it completely dissolved. Thereafter, 8.5 g of TEOS was added, and the mixture was kept stirring at 40 °C for 24 h. Then, the solution was transferred to a 200 mL autoclave and aged at 120 °C for another 24 h. Finally, the resultant solution was evaporated in a rotating evaporator under 60 °C and calcined at 550 °C in air for 6 h. The obtained sample was defined as *n*Ca/SBA-15, where *n* represents the Ca/Si atomic ratio.

For comparison, another series of Ca/SBA-15 samples were obtained by an impregnation method, and the synthesis schematic was as follows. SBA-15 was synthesized as above; then the mixture of $Ca(NO_3)_2$ and SBA-15 with different atomic ratios was stirred using deionized water as agent at 40 °C for 24 h. The resultant mixture was dried at 60 °C in a rotating evaporator and finally calcined at 550 °C in air for 6 h. The obtained sample synthesized by impregnation method was defined as *n*Ca/SBA-15-IM, where *n* represents the Ca/Si atomic ratio.

Characterization of Catalysts

XRD analysis was performed on a Bruker D8 Advance diffractometer using Cu $K_{\alpha 1}$ radiation, in the 2θ range of 0.5°–4.0° at 40 kV and 100 mA. FTIR spectra of the samples were obtained in the wavenumber region of 400–4000 cm^{-1} on a Nicolet 380 spectrophotometer by using a standard KBr technique. TEM analysis was carried on a Zeiss Libra 200 FE electron microscope operated at 200 kV. N_2 physisorption was measured using a Quantachrome Autosorb-IQ gas adsorption analyzer. Then the surface area was obtained by BET equation, and pore size distributions were determined from the isotherm of adsorption using the BJH method. TGA was carried out using STA 449 F3 thermal analysis machine under a flow of air in the temperature range of 50 °C to 800 °C with a heating rate of 10 °C/min. The basicity of these samples was studied by CO_2-TPD on a Chembet Pulsar temperature-programmed reduction/TPD (TPR/TPD) apparatus. About 50 mg of catalysts were pretreated under a flow of Ar at 500 °C for 1.5 h. Then, temperature was decreased down to room temperature, and CO_2 adsorption was carried out at 50 °C for 1.5 h. Thereafter, the physisorbed CO_2 was removed by a flushing with Ar. TPD was carried out in the stream of Ar (20 mL/min) at a heating rate of 10 °C/min up to 800 °C, and CO_2 was detected by an on-line gas chromatograph provided with a thermal conductivity detector (TCD).

Synthesis of PCs

PIC samples were synthesized by a one-pot method, including transesterification and polycondensation. A generalized procedure is described below. DPC (10.71 g, 50 mmol), ISB (7.31 g, 50 mmol) and 0.4Ca/SBA-15 (0.002 g, 0.02 wt% based on DPC) were successively added to a 50 mL three-necked flask equipped with a mechanical stirrer, reflux condenser, N_2 inlet and thermometer. In the transesterification stage, the reaction temperature was increased to 180 °C under N_2 atmosphere, which was maintained for 30 min. Next the pressure in flask was gradually reduced to 200 Pa and kept for 20 min to remove volatile by-products. During the polycondensation stage, the temperature was increased to 240 °C, and the reaction was maintained for 60 min under high vacuum (< 200 Pa). Finally, the PIC sample was obtained by dissolving in dichloromethane and precipitating with alcohol. Other PCs including poly(propylene carbonate) (PPC), poly(butylene carbonate) (PBC), poly(pentamethylene carbonate) (PMC), poly(hexamethylene carbonate) (PHC), bisphenol-A polycarbonate (BPA-PC) and poly(butylene-*co*-isosorbide carbonate)

https://doi.org/10.1007/s10118-018-2137-4

(PBIC) were also synthesized *via* the same procedure.

Characterization of PCs

The intrinsic viscosities (η) of the PCs were investigated by Ubbelohde viscometer using dichloromethane as an agent at 25 °C. The M_w and polydispersity index (PDI = M_w/M_n) were determined by Agilent PL-GPC 50 system equipped with a refractive index detector, a G1312A pump and a column (PLgel MIXED-C) oven temperature of 30 °C. Chloroform was used as the eluent (1.0 mL/min), and polystyrene standards were used to establish a calibration curve. The glass transition temperature (T_g) of polymers was determined by DSC using the instrument DSC-Q20 at a heating rate of 10 °C/min with a N_2 gas purge (50 mL/min). TGA data were acquired with a STA 449 F3 thermal analysis machine under a N_2 flow rate of 20 mL/min by heating samples (3.0 mg) from 50 °C to 600 °C at a rate of 10 °C/min. The yield was expressed in percent of the theoretical value, which was calculated based on the 100% conversion of ISB to PIC.

RESULTS AND DISCUSSION

Catalyst Screening for the Transesterification of DPC with ISB

The catalytic tests of Ca/SBA-15 samples for the melt transesterification of DPC with ISB were performed at given conditions. Fig. S1 (in electronic supplementary information, ESI) exhibits GPC traces of PIC samples synthesized by different catalysts, respectively. The data of η, M_w and PDI of PIC samples are summarized in Table 1. Compared to SBA-15, the catalytic activities can be obviously enhanced on the introduction of calcium. One can see that the η and M_w values of PIC over Ca/SBA-15 are significantly increased as increasing Ca/Si atomic ratios from 0 to 0.4. Further increasing Ca/Si atomic ratios over 0.4 would slightly lessen the η and M_w values for the obtained PIC, and the highest η and M_w value of 57.9 mL/g and 4.41 × 10^4 g/mol can be obtained by using 0.4Ca/SBA-15 as catalyst. It is worthy noting that the catalytic activity of 0.4Ca/SBA-15-IM has a sharp decline compared with 0.4Ca/SBA-15. In addition, the yield of PIC over Ca/SBA-15 is obviously enhanced as increasing Ca/Si atomic ratio from 0 to 0.2. But there is no obvious difference in yield when Ca/Si atomic ratio exceeds 0.2. As shown in Table 1, PIC obtained over 0.4Ca/SBA-15 has the highest η, M_w and yield values. Obviously, 0.4Ca/SBA-15 should be the best catalyst and further investigations were carried out.

Optimization of the Reaction Conditions

In order to obtain the optimum conditions for 0.4Ca/SBA-15 catalyst, the influence of various reaction parameters was studied. Fig. 1(a) shows the impact of the catalyst concentration on PIC synthesis with the amount of 0.4Ca/SBA-15 varied from 0.005 wt% to 0.05 wt% (respect to the mass of DPC). It is clearly showed that the catalyst amount significantly enhances the η and yield of PIC when the catalyst amount is at a low concentration. Thereafter, no remarkable improvement for the η and yield values of PIC is observed when the catalyst amount exceeds 0.02 wt%. Comprehensive consideration, the optimum amount of catalyst is 0.02 wt% for 0.4Ca/SBA-15 in this process.

The effect of polymerization temperature on PIC synthesis is investigated in the range of 200−260 °C. As shown in Fig. 1(b), the η value of PIC is sharply increased with raising the reaction temperature from 200 °C to 240 °C, followed by a gradual decrease between 250 and 260 °C. It is easily understood that this reaction process is a typical reverse reaction consisting of polymerization and decomposition. When the reaction temperature changes from 200 °C to 240 °C, polymerization plays a leading role. Moreover, increasing temperature decreases polymer viscosity, which can promote polymerization reaction[21, 23, 37]. When the temperature exceeds 240 °C, decomposition plays a dominant role, which results in side reactions. In addition, when the polymerization temperature is 240 °C, the yield of PIC reaches its maximum. Evidently, 240 °C should be a suitable polymerization temperature for 0.4Ca/SBA-15 catalyst considering its η and yield value comprehensively.

Finally, the effects of polycondensation time on PIC synthesis is also investigated at 240 °C. As shown in Fig. 1(c), the η value reaches 28.3 mL/g after 15 min and the yield value reaches 83.2%. As reaction proceeds, the η speedily increases to 65.9 mL/g with corresponding M_w of 4.88 × 10^4 g/mol when the polycondensation time is up to 75 min. However, further prolonging the polycondensation time leads to the decrease of η value. This phenomenon can be ascribed to the fact that excessive reaction time could enhance its reverse reaction, which also has been observed in other works[21–23]. In the present study, the highest M_w value of PIC over 0.4Ca/SBA-15 is 4.88 × 10^4 g/mol which is much higher than those for LiAcac[21], Cs_2CO_3[22] and TEAI[23] in the same reaction reported in earlier papers.

Substrate Scope

To develop the general application range of 0.4Ca/SBA-15 catalyst, the catalytic performance of DPC with a series of diol substrates, including 1,3-propanediol (PD), 1,4-butanediol (BD), 1,5-pentanediol (MD), 1,6-hexanediol (HD), bisphenol A (BPA) and ISB/BD (molar ratio 1:1) for

Table 1 Catalytic performance of Ca/SBA-15 for the melt transesterification of DPC with ISB [a]

Entry	Catalyst	η (mL/g)	M_w × 10^{-4} (g/mol)	PDI	Yield (%)
1	SBA-15	25.5	1.51	1.63	67.4
2	0.1Ca/SBA-15	40.9	2.85	1.63	82.4
3	0.2Ca/SBA-15	45.1	3.40	1.72	87.7
4	0.3Ca/SBA-15	49.3	3.96	1.86	94.0
5	0.4Ca/SBA-15	57.9	4.41	1.64	95.0
6	0.5Ca/SBA-15	54.0	4.20	1.73	94.5
7	0.4Ca/SBA-15-IM	41.7	2.93	1.86	90.5

[a] Reaction conditions: catalyst (0.02 wt%), 240 °C, 200 Pa, 1 h (condensation stage)

https://doi.org/10.1007/s10118-018-2137-4

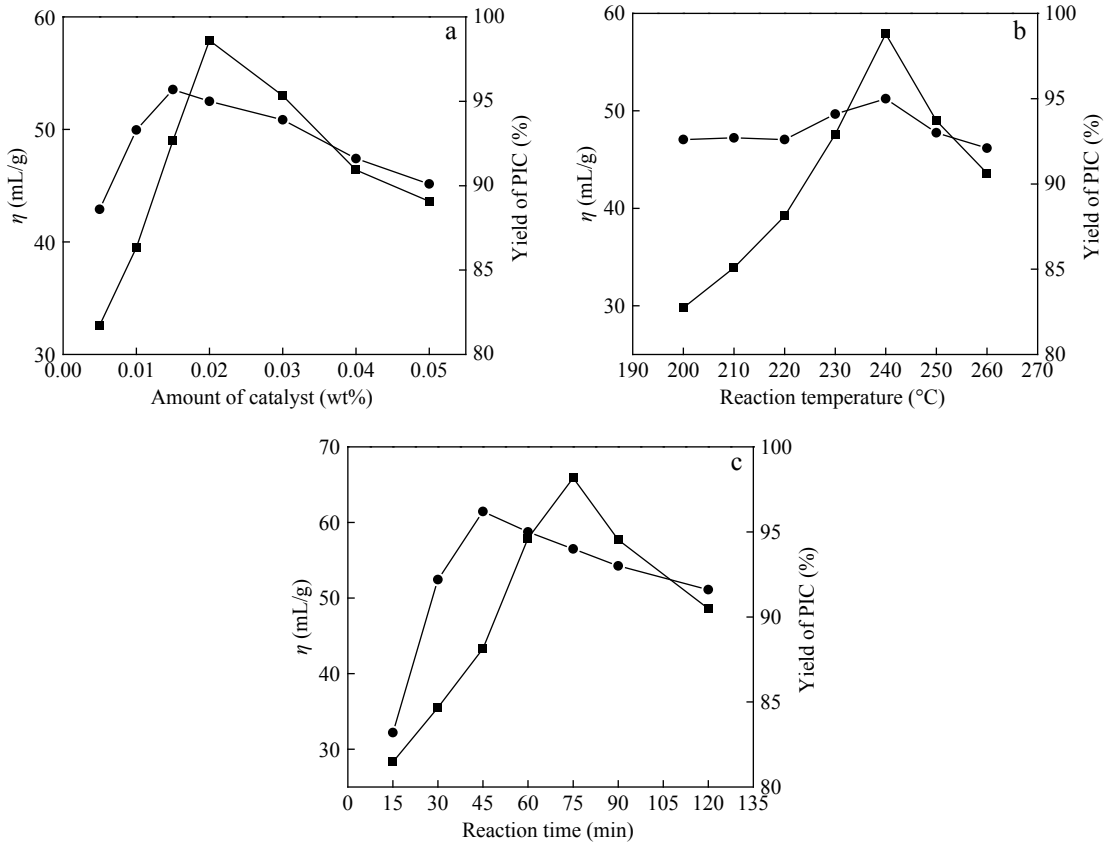

Fig. 1 Effects of reaction conditions on η (■) and yield (●) of PIC over 0.4Ca/SBA-15: influence of (a) amount of catalyst (240 °C, 1 h), (b) polymerization temperature (0.02 wt%, 1 h) and (c) polymerization time (0.02 wt%, 240 °C)

the synthesis of corresponding poly(propylene carbonate) (PPC), poly(butylene carbonate) (PBC), poly(pentamethylene carbonate) (PMC), poly(hexamethylene carbonate) (PHC), bisphenol-A polycarbonate (BPA-PC) and poly(butylene-*co*-isosorbide carbonate) (PBIC), are also investigated. As shown in Table 2, other diols, especially aliphatic diols, can also easily transesterificate with DPC to synthesize PCs with a considerable M_w. In comparison with other catalysts, such as TSP-44[38, 39], BMIM-2-CO_2[40], metallic oxide[37, 41], and alkali metal acetylacetonates[41], 0.4Ca/SBA-15 has a comparable activity for this process. The M_w of APCs obtained by 0.4Ca/SBA-15 are higher than 7.00×10^4, which can satisfy the demand of M_w for biodegradable plastics[38].

Thermal Properties of PIC

The thermal properties of the PIC samples are evaluated by DSC and TGA, with the results shown in Table 3. Fig. 2 shows the DSC traces of these samples. They are found to be in an amorphous state as a result of the unsymmetrical carbonate linkages between repeat units[23]. Interestingly, 0.4Ca/SBA-15 generates a PIC with the highest T_g of 169 °C among these catalysts. Compared with other PIC samples, the highest T_g observed in PIC-0.4Ca/SBA-15 sample is mostly because of the highest M_w, as explained in other work[22].

TGA and DTG curves of PIC are depicted in Fig. 3. Apparently, PIC samples degrade only in a single step. Fig. 3 indicates that the degradation peak of the PIC-0.4Ca/SBA-15

Table 2 Catalytic performance of 0.4Ca/SBA-15 for the melt transesterification of DPC with other diols [a]

Entry	Sample	η (mL/g)	$M_w \times 10^{-4}$ (g/mol)	PDI	Yield (%)
1	PIC	57.9	4.41	1.64	95.0
2 [b]	PPC	19.5	1.03 [d]	1.64	55.9
3 [b]	PBC	72.3	5.67 [d]	1.71	78.9
4	PBC	96.4	8.11 [d]	1.67	75.6
5	PMC	84.3	7.57 [d]	1.84	80.3
6	PHC	83.2	7.44 [d]	1.83	85.2
7	BPA-PC	18.6	0.95 [d]	1.41	90.4
8 [c]	PBIC	86.7	7.58	1.65	86.3

[a] Reaction conditions: the molar ratio of diols/DPC was 1:1, catalyst (0.02 wt%), 180 °C, 1.01×10^5 Pa, 1 h (transesterification stage), 240 °C, 200 Pa, 1 h (condensation stage); [b] The reaction was carried out at 210 °C for 1.0 h; [c] The molar ratio of ISB/BD was 1:1; [d] Determined by GPC in tetrahydrofuran (1.0 mL/min) at 30 °C

https://doi.org/10.1007/s10118-018-2137-4

Table 3 Thermal properties of different PIC samples

Entry	Sample	$M_w \times 10^{-4}$ (g/mol)	PDI	T_g [a] (°C)	$T_{5\%}$ [b] (°C)	T_{max} [b] (°C)
1	PIC-SBA-15	1.51	1.63	152	328	369
2	PIC-0.4Ca/SBA-15	4.88	1.59	169	333	373
3	PIC-0.4Ca/SBA-15-IM	2.93	1.86	163	332	370

[a] Determined by DSC measurements at a heating rate of 10 °C/min (second heating); [b] $T_{5\%}$ and T_{max} determined by TGA under N_2 at a heating rate of 10 °C/min

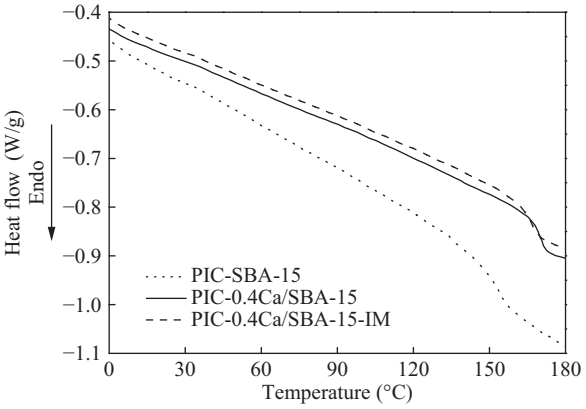

Fig. 2 DSC traces of different PIC samples

sample shifts to a higher temperature region. As expected, the thermal stability of PIC is improved with increasing M_w[21, 22]. Table 3 summarizes the T_d values of the samples at 5% weight loss ($T_{5\%}$) and the maximum degradation rate (T_{max}). The PIC-0.4Ca/SBA-15 sample displays a remarkably highest $T_{5\%}$ of 333 °C and T_{max} of 373 °C. Based on the observed T_g, $T_{5\%}$ and T_{max}, 0.4Ca/SBA-15 is a good catalyst for the melt polymerization of ISB and DPC.

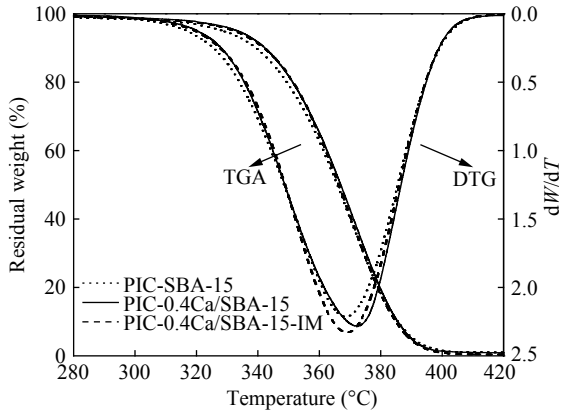

Fig. 3 TGA and DTG curves of different PIC samples

Results of Catalyst Characterization

Small-angle XRD patterns of Ca/SBA-15 samples are illustrated in Fig. 4. The diffraction peaks of all catalyst samples are well in accordance with the standard diffraction of ordered mesoporous SBA-15, which shows Ca/SBA-15 perseveres an optimal ordering of the 2D-hexagonal P6mm structure[43]. Fig. 4(a) shows that the intensity of all reflections decrease along with calcium content increase, as explained in other works that the introduction of metal oxides decreases the thickness of pore walls and pore space of mesoporous silicon[33, 35]. Fig. 4(b) displays that small-

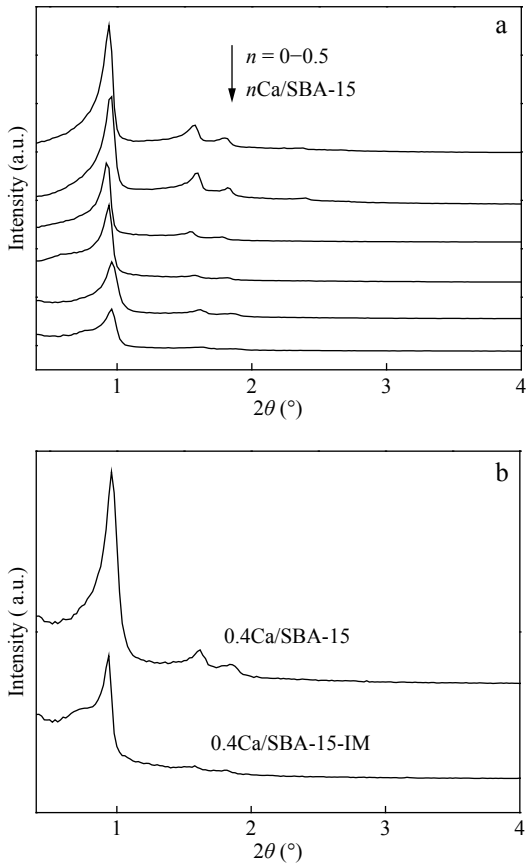

Fig. 4 Small-angle XRD patterns of (a) *n*Ca/SBA-15 (n = 0–0.5), (b) 0.4Ca/SBA-15 and 0.4Ca/SBA-15-IM

angle XRD intensity of 0.4Ca/SBA-15 is much stronger than that of 0.4Ca/SBA-15-IM, which implies that the ordered mesopores are more easily persevered by a one-pot route[34, 35].

FTIR spectra of Ca/SBA-15 samples are displayed in Fig. S2 (in ESI). Several broad transmission bands at approximately 3440, 1636, and a range of 1050–1100 cm^{-1} appear in the spectra of all catalyst samples. The bands at approximately 3440 and 1636 cm^{-1} are due to the OH, the former for OH stretching vibration and the latter for the bending mode of physically adsorbed water[44]. The band in the range of 1050–1100 cm^{-1} is assigned to vibration of Si—O bond[45, 46]. Moreover, as shown in Fig. S2(a) (in ESI), the increase of calcium content would increase the intensity of both OH^- groups[47]. In addition, two new peaks at 1498 and 1438 cm^{-1} are found in the spectra of 0.3–0.5Ca/SBA-15 samples, which are attributed to CO_3^{2-} symmetric stretching vibration band[47]. Fig. S2(b) (in ESI) shows the FTIR spectra of 0.4Ca/SBA-15 and 0.4Ca/SBA-15-IM. It is noteworthy that a sharp peak develops at

1390 cm^{-1} in the spectrum of 0.4Ca/SBA-15-IM, which could be ascribed to the vibration of N—O of nitrate[33]. This is probably attributed to the incomplete decomposition of $Ca(NO_3)_2$. In addition, the intensities of OH group and Si—O bond detected on 0.4Ca/SBA-15 are much higher than those of 0.4Ca/SBA-15-IM, which indicates that these functional groups are much easily formed on the surface of mesoporous silicon by a one-pot route[35].

Fig. S3 (in ESI) depicts the N_2 adsorption-desorption isotherms of Ca/SBA-15 samples. These samples all display type IV with H1 hysteresis loop, which proves Ca/SBA-15 samples have ordered mesoporous structures similar to SBA-15. As shown in Fig. S3(a) (in ESI), although the amount of adsorbed N_2 decreases along with the increase of calcium content, the position of the inflections slightly shifts toward smaller p/p_0 values. From the data of physicochemical properties listed in Table 4, the S_{BET} and pore volume are decreased with increasing Ca/Si atomic ratio from 0 to 0.5, which is in agreement with previous work[30, 34]. As shown in Fig. S3(b) (in ESI) and Table 4, there are no remark differences in S_{BET} and pore volume between 0.4Ca/SBA-15 and 0.4Ca/SBA-15-IM.

Table 4 Physicochemical characteristics of different Ca/SBA-15 catalysts

Catalyst	S_{BET} (m^2/g)	Pore diameter (nm)	Pore volume (cm^3/g)
SBA-15	535.6	9.9	0.94
0.1Ca/SBA-15	407.6	9.4	0.71
0.2Ca/SBA-15	341.6	9.2	0.72
0.3Ca/SBA-15	282.5	9.3	0.67
0.4Ca/SBA-15	172.2	9.5	0.63
0.5Ca/SBA-15	152.3	9.0	0.44
0.4Ca/SBA-15-IM	168.6	9.3	0.62

Fig. 5 shows the representative TEM images of SBA-15, 0.4Ca/SBA-15 and 0.4Ca/SBA-15-IM samples. TEM images display a regular hexagonal array of uniform channel characteristics preserved in these samples, which are in accordance with the results of XRD and N_2 adsorption. The surface of 0.4Ca/SBA-15 is much like that of SBA-15, which indicates that calcium is formatted as a smooth layer on the surface of SBA-15. Nevertheless, the surfaces of 0.4Ca/SBA-15-IM seem to be covered by clouds which are caused by the overloading of calcium[33]. This phenomenon demonstrates that Ca/SBA-15 synthesized by one-pot route can get a better calcium dispersion, which keeps pace with XRD, FTIR, and N_2 adsorption-desorption isotherms.

The TGA and DTG curves of SBA-15, 0.4Ca/SBA-15 and 0.4Ca/SBA-15-IM samples before calcination are shown in Fig. S4 (in ESI). As shown in Fig. S4(a) (in ESI), the weight losses of un-calcined SBA-15 are concentrated in the range of 150−270 °C, which could be assigned to the decomposition of P123. As displayed in Figs. S4(b) and S4(c) (in ESI), the TGA curves of the un-calcined 0.4Ca/SBA-15 and 0.4Ca/SBA-15-IM sample are concentrated in two ranges: the first range 50−120 °C is ascribed to the loss of physical adsorbed H_2O, the second rang 150−600 °C is assigned to the decomposition of P123

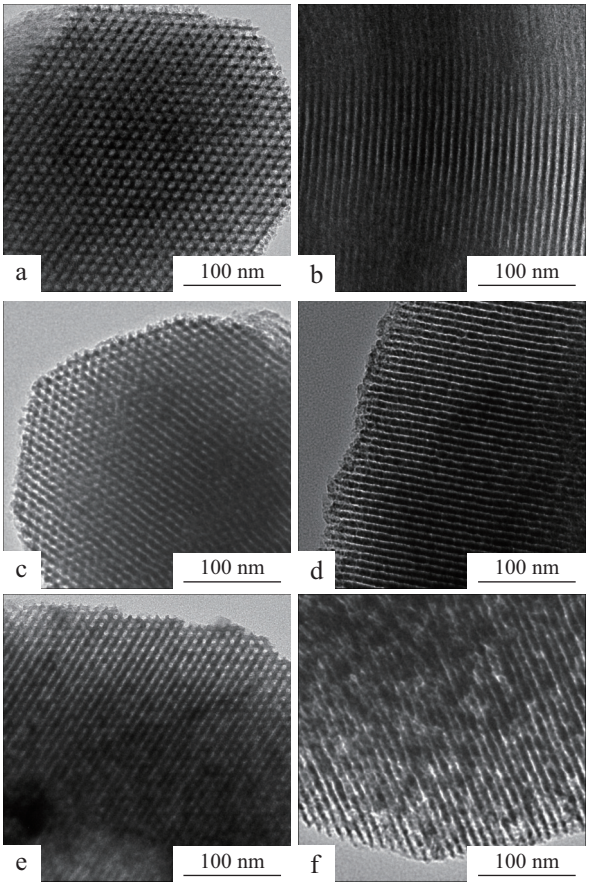

Fig. 5 TEM images of (a, b) SBA-15, (c, d) 0.4Ca/SBA-15 and (e, f) 0.4Ca/SBA-15-IM

and $Ca(NO_3)_2$. Compared with the TGA curve of un-calcined 0.4Ca/SBA-15, the second range of un-calcined 0.4Ca/SBA-15-IM is concentrated in the range of 400−600 °C, which is ascribed to the decomposition of $Ca(NO_3)_2$. It is worth noting the DTG curves of un-calcined 0.4Ca/SBA-15 show several maxima at 250−400 °C, which is not detected in those of un-calcined SBA-15 and 0.4Ca/SBA-15-IM. It may be caused by a lower temperature for the decomposition of $Ca(NO_3)_2$ taking place in Ca/SBA-15[34].

The basic site strength and amount of these catalysts are determined by CO_2-TPD, and the results are listed in Table 5. According to the literature[31], the amount of weak, medium and strong basic sites can be expressed in mol desorbed CO_2/g over the range of 50−150, 150−500, and > 500 °C, respectively. It is clearly seen that both the total amount of basic site and basicity strength increase with increasing calcium. The CO_2-TPD profiles of SBA-15, 0.4Ca/SBA-15 and 0.4Ca/SBA-15-IM samples are displayed in Fig. 6. Only one CO_2 desorption peak at 150 °C can be observed for weak basic sites in SBA-15, which is ascribed to the interaction of CO_2 with SiO_2. Compared with SBA-15, 0.4Ca/SBA-15-IM exhibits a sharp peak at 500 °C for strong basic sites, which implies the adsorption of CO_2 on the surface of isolated CaO[30]. It is worth noting that 0.4Ca/SBA-15 shows a varied form of basic sites in contrast with 0.4Ca/SBA-15-IM, which reveals more medium basic sites have been formed by one-pot route. These medium basic sites are probably caused by

https://doi.org/10.1007/s10118-018-2137-4

Table 5 Surface basicity of different Ca/SBA-15 catalysts

Catalyst	Desorption peaks (area%)			Total evolved CO_2 (μmol/g)
	Weak	Medium	Strong	
SBA-15	35.1	64.9	0	30.6
0.1Ca/SBA-15	30.6	67.0	2.4	49.1
0.2Ca/SBA-15	23.3	72.3	4.4	69.2
0.3Ca/SBA-15	20.4	73.3	6.3	83.5
0.4Ca/SBA-15	17.2	75.7	7.1	104.1
0.5Ca/SBA-15	15.8	75.9	8.3	125.2
0.4Ca/SBA-15-IM	8.1	51.7	40.2	107.9

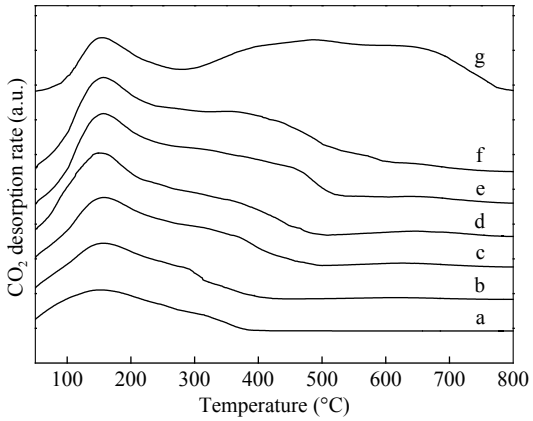

Fig. 6 CO_2-TPD profiles of (a) SBA-15, (b) 0.1Ca/SBA-15, (c) 0.2Ca/SBA-15, (d) 0.3Ca/SBA-15, (e) 0.4Ca/SBA-15, (f) 0.5Ca/SBA-15 and (g) 0.4Ca/SBA-15-IM

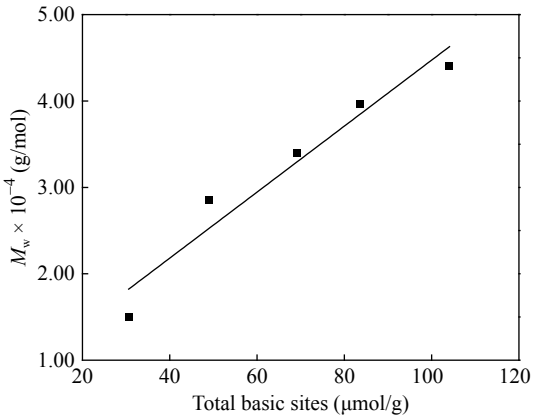

Fig. 7 Effect of surface basicity on catalytic activity for Ca/SBA-15 catalysts. Reaction conditions: catalyst (0.02 wt%), 200 Pa, 1 h (condensation stage)

the adsorption of CO_2 on the surface of $CaSiO_3$ species[35]. The different basic species generated in SBA-15 are mainly attributed to the varied quantity of Si—OH groups on the surface of silica framework before Ca^{2+} activation. In a one-pot route, many Si—OH groups are preserved on the surface of silica framework before calcinations. After being activated, Ca^{2+} is easily reacted with silica species to form $CaSiO_3$[34]. For the impregnation method, on account of the loss of surface Si—OH groups at the first step calcinations, the main reaction occurring on the surface of SBA-15 is the decomposition of $Ca(NO_3)_2$ with a product of CaO[31, 32].

Possible Reaction Mechanism

According to the literatures[48, 49], the basicity, S_{BET} and pore structure are the critical factors for the solid base in transesterification reaction. Therefore, the relation between these physicochemical properties of catalysts and the η, M_w, and yield value of PIC has been discussed. As shown in Tables 1 and 4, the physical structure of S_{BET} and pore structure do not exert an clear effect on the η, M_w, and yield value of PIC, implying that the S_{BET} and pore structure are not the most critical factors for this reaction. This can be explained by the fact that high molecular weight limits the diffusion of the reactant in the catalysts[41]. Additionally, one also can see from Tables 1 and 5 that the increase of basic site amount seems to be advantageous to the improvement of η, M_w, and yield value of PIC. In order to further confirm this conclusion, the effect of surface basicity on catalytic activity for Ca/SBA-15 samples is displayed in Fig. 7. When the total basic sites of Ca/SBA-15 are in the range of 30.6 μmol/g to 104.1 μmol/g, increasing total basic sites significantly enhances M_w. The 0.4Ca/SBA-15 generates a polymer with the highest M_w. Compared with 0.4Ca/SBA-15, 0.5Ca/SBA-15 shows slightly lower catalytic performance although it has more Ca content and basic sites. This can be reasoned by their low S_{BET} and small pore size, because the increase of basic sites and the decrease of S_{BET} and pore size can compensate each other, thus generating the maximum M_w of PIC for 0.4Ca/SBA-15.

In order to further give insight into the surface basicity of catalysts in relation to its activity, 0.4Ca/SBA-15-IM with strong basic sites was prepared by an impregnation method. It is worth noting that there is no remark difference in the amount basic sites between 0.4Ca/SBA-15 and 0.4Ca/SBA-15-IM, but the M_w of PIC obtained over 0.4Ca/SBA-15 is much higher than that of 0.4Ca/SBA-15-IM. The strong basic sites in the surface of 0.4Ca/SBA-15-IM would give a negative effect on the increase of M_w by promoting PIC depolymerization and decomposition[37]. As discussed above, the basic site strength and amounts play an important role in this reaction, and the weak and medium basic sites produce a positive impact on the polymerization reaction.

CONCLUSIONS

In this work, Ca/SBA-15 samples prepared by two methods were used as catalyst for the transesterification of DPC and ISB to synthesize high-molecular-weight PIC. The catalytic activity of Ca/SBA-15 is mainly influenced by the amount and strength of basic sites, which can be changed by using various synthetic methods and choosing different Ca/Si atomic ratios. Moreover, strong basic sites were found to

https://doi.org/10.1007/s10118-018-2137-4

promote the decomposition of the resultant PIC. Thereafter, 0.4Ca/SBA-15 was detected to be the best catalyst for this process, resulting in PIC polymer with M_w of 4.88 × 10^4 g/mol and T_g of 169 °C at its optimal conditions. In addition, Ca/SBA-15 was also found to catalyze the transerification of DPC with other diols to synthesize corresponding PCs.

Electronic Supplementary Information

Electronic supplementary information (ESI) is available free of charge in the online version of this article at http://dx.doi.org/10.1007/s10118-018-2137-4.

ACKNOWLEDGMENTS

This work was financially supported by the National Key R&D Program of China (No. 2016YFB0301900) and the Science and Technology Support Program of Sichuan Province (No. 2015GZ0065).

REFERENCES

1 Oyarzabal, A.; Cristiano-Tassi, A.; Laredo, E.; Newman, D.; Bello, A.; Etxeberría, A.; Eguiazabal, J. I.; Zubitur, M.; Mugica, A.; Müller, A. J. Dielectric, mechanical and transport properties of bisphenol A polycarbonate/graphene nanocomposites prepared by melt blending. J. Appl. Polym. Sci. 2017, 134(13), 44654−44667.
2 Zhao, H. M.; Jiang, M. J.; Tian, H. S. NaOH and TEAH catalyzed polycarbonate synthesis through melt transesterification and the rearrangement prodouts in both processes. Acta Polymerica Sinica (in Chinese) 2011, (2), 192−197.
3 Song, Q. L.; Wen, H. Y.; Christiansen, J. D.; Yu, D. H.; Chen, C. S.; Jiang, S. C. Analysis of structure transition and compatibility of PTT/PC blend without transesterification. Chinese J. Polym. Sci. 2016, 34(9), 1172−1182.
4 Hao, Y. P.; Yang, H. L.; Zhang, G. B.; Zhang, H. L.; Gao, G.; Dong, L. S. Rheological, thermal and mechanical properties of biodegradable poly(propylene carbonate)/polylactide/poly(1,2-propylene glycol adipate) blown films. Chinese J. Polym. Sci. 2015, 33(12), 1702−1712.
5 Geens, T.; Aerts, D.; Berthot, C.; Bourguignon, J. P.; Goeyens, L.; Lecomte, P.; Maghuin-Rogister, G.; Pironnet, A. M.; Pussemier, L.; Scippo, M. L. A review of dietary and non-dietary exposure to bisphenol-A. Fd. Chem. Toxicol. 2012, 50(10), 3725−3740.
6 Gubbels, E.; Jasinska-Walc, L.; Koning, C. E. Synthesis and characterization of novel renewable polyesters based on 2,5-furandicarboxylic acid and 2,3-butanediol. J. Polym. Sci., Part A: Polym. Chem. 2013, 51(4), 890−898.
7 Li, C.; Dai, J. Y.; Liu, X. Q.; Jiang, Y. H.; Ma, S. Q.; Zhu, J. Green synthesis of a bio-based epoxy curing agent from isosorbide in aqueous condition and shape memory properties investigation of the cured resin. Macromol. Chem. Phys. 2016, 217(13), 1439−1447.
8 Wang, J. G.; Liu, X. Q.; Zhang, Y. J.; Liu, F.; Zhu, J. Modification of poly(ethylene 2,5-furandicarboxylate) with 1,4-cyclohexanedimethylene: Influence of composition on mechanical and barrier properties. Polymer 2016, 103, 1−8.
9 Deng, J.; Liu, X. Q.; Li, C.; Jiang, Y. H.; Zhu, J. Synthesis and properties of a bio-based epoxy resin from 2,5-furandicarboxylic acid (FDCA). RSC Adv. 2015, 5(21), 15930−15939.
10 Dai, J. Y.; Ma, S. Q.; Teng, N.; Dai, X. Y.; Shen, X. B.; Wang, S.; Liu, X. Q.; Zhu, J. 2,5-Furandicarboxylic acid- and itaconic acid-derived fully biobased unsaturated polyesters and their cross-linked networks. Ind. Eng. Chem. Res. 2017, 56(10), 2650−2657.
11 Kricheldorf, H. R. "Sugar diols" as building blocks of polycondensates. J. Macromol. Sci. Rev. Macromol. Chem. Phys. 1997, C37(4), 599−631.
12 Fenouillot, F. F.; Rousseau, A.; Colomines, G.; Saint-Loup, R.; Pascault, J. P. Polymers from renewable 1,4:3,6-dianhydrohexitols (isosorbide, isomannide and isoidide): A review. Prog. Polym. Sci. 2010, 35(5), 578−622.
13 Bersot, J. C.; Jacquel, D.; Saint-Loup, P.; Fuertes, P.; Rousseau, A.; Pascault, J. P.; Spitz, R.; Fenouillot, F.; Monteil, V. Efficiency increase of poly(ethylene terephthalate-*co*-isosorbide terephthalate) synthesis using bimetallic catalytic systems. Macromol. Chem. Phys. 2011, 212(19), 2114−2120.
14 Gioia, C.; Vannini, M.; Marchese, P.; Minesso, A.; Cavalieri, R.; Colonna, M.; Celli, A. Sustainable polyesters for powder coating applications from recycled PET, isosorbide and succinic acid. Green Chem. 2014, 16(4), 1807−1815.
15 Caouthar, A. A.; Loupy, A.; Bortolussi, M.; Blais, J. C.; Dubreucq, L.; Meddour, A. Synthesis and characterization of new polyamides based on diphenylaminoisosorbide. Polym. Chem. 2005, 43(24), 6480−6491.
16 Wroblewska, A.; Zych, A.; Thiyagarajan, S.; Dudenko, D.; van Es, D.; Hansen, M. R.; Koning, C.; Duchateau, R.; Jasinska-Walc, L. Towards sugar-derived polyamides as environmentally friendly materials. Polym. Chem. 2015, 6(22), 4133−4143.
17 Lee, C. H.; Kato, M.; Usuki, A. Preparation and properties of bio-based polycarbonate/clay nanocomposites. J. Mater. Chem. A 2011, 21(19), 6844−6847.
18 Chatti, S.; Schwarz, S.; Kricheldorf, H. R. Crclic and noncylic polycarbonates of isosorbide (1,4:3,6-dianhydro-D-glucitol). Macromolecules 2006, 39(26), 9064−9070.
19 Feng, L.; Zhu, W. X.; Li, C. C.; Guan, G. H.; Zhang, D.; Xiao, Y. N.; Zheng, L. C. A high-molecular-weight and high-T_g poly(ester carbonate) partially based on isosorbide: synthesis and structure-property relationships. Polym. Chem. 2014, 6(4), 633−642.
20 Park, J. H.; Jeon, J. Y.; Lee, J. J.; Jang, Y.; Varghese, J. K.; Lee, B. Y. Preparation of high-molecular-weight aliphatic polycarbonates by condensation polymerization of diols and dimethyl carbonate. Macromolecules 2013, 46(9), 3301−3308.
21 Li, Q.; Zhu, W. X.; Li, C. C.; Guan, G. H.; Zhang, D.; Xiao, Y. N.; Zheng, L. C. A non-phosgene process to homopolycarbonate and copolycarbonates of isosorbide using dimethyl carbonate: synthesis, characterization, and properties. J. Polym. Sci., Part A: Polym. Chem. 2013, 51(6), 1387−1397.
22 Eo, Y. S.; Rhee, H. W.; Shin, S. H. Catalyst screening for the melt polymerization of isosorbide-based polycarbonate. J. Ind. Eng. Chem. 2016, 37, 42−46.
23 Sun, W.; Xu, F.; Cheng, W. G.; Sun, J.; Ning, G. Q.; Zhang, S. J. Synthesis of isosorbide-based polycarbonates via melt polycondensation catalyzed by quaternary ammonium ionic liquids. Chin. J. Catal. 2017, 38(5), 908−917.
24 Chrysanthos, M.; Galy, J.; Pascault, J. P. Preparation and properties of bio-based epoxy networks derived from isosorbide diglycidyl ether. Polymer 2011, 52, 3611−3620.
25 Hu, F. S.; La Scala, J. J.; Sadler, J. M.; Palmese, G. R. Synthesis and characterization of thermosetting furan-based epoxy systems. Macromolecules 2014, 47(10), 3332−3342.
26 Li, C.; Dai, J. Y.; Liu, X. Q.; Jiang, Y. H.; Ma, S. Q.; Zhu, J. Green Synthesis of a bio-based epoxy curing agent from isosorbide in aqueous condition and shape memory properties investigation of the cured resin. Macromol. Chem. Phys. 2016, 217(13), 1439−1447.
27 Zhao, D. Y.; Feng, J. L.; Huo, Q. S.; Melosh, N.; Fredrickson,

G. H.; Chmelka, B. F.; Stucky, G. D. Triblock copolymer syntheses of mesoporous silica with periodic 50 to 300 angstrom pores. Science 1998, 279(5350), 548−552.
28 Zhao, D. Y.; Huo, Q. S.; Feng, J. L.; Chmelka, B. F.; Stucky, G. D. Nonionic triblock and star diblock copolymer and oligomeric surfactant syntheses of highly ordered, hydrothermally stable, mesoporous silica structures. J. Am. Chem. Soc. 1998, 120(24), 6024−6036.
29 Chen, S. Y.; Huang, C. Y.; Yokoi, T.; Tang, C. Y.; Huang, S. J.; Lee, J. J.; Chan, J. C. C.; Tatsumi, T.; Cheng, S. Synthesis and catalytic activity of amino-functionalized SBA-15 materials with controllable channel lengths and amino loadings. J. Mater. Chem. 2012, 22(5), 2233−2243.
30 Liu, X. Y.; Sun, L. B.; Lu, F.; Liu, X. D.; Liu, X. Q. Low-temperature generation of strong basicity via an unprecedented guest-host redox interaction. Chem. Commun. 2013, 49(73), 8087−8089.
31 Albuquerque, M. C. G.; Jiménez-Urbistondo, I.; Santamaría-González, J.; Mérida-Robles, J. M.; Moreno-Tost, R.; Rodríguez-Castellón, E.; Jiménez-López, A.; Azevedo, D. C. S.; Cavalcante, C. L.; Maireles-Torres, P. CaO supported on mesoporous silicas as basic catalysts for transesterification reactions. Appl. Catal. A-Gen. 2008, 334(1-2), 35−43.
32 Sun, L. B.; Kou, J. H.; Chun, Y.; Yang, J.; Gu, F. N.; Wang, Y.; Zhu, J. H.; Zou, Z. G. New attempt at directly generating superbasicity on mesoporous silica SBA-15. Inorg. Chem. 2008, 47(10), 4199−4208.
33 Arumugam, A.; Ponnusami, V. Optimization of recovery of silica from sugarcane leaf ash and Ca/SBA-15 solid base for transesterification of Calophyllum inophyllum oil. J. Sol-Gel. Sci. Technol. 2015, 74(1), 132−142.
34 Tantirungrotechai, J.; Thananupappaisal, P.; Yoosuk, B.; Viriya-empikul, N.; Faungnawakij, K. One-pot synthesis of calcium-incorporated MCM-41 as a solid base catalyst for transesterification of palm olefin. Catal. Commun. 2011, 16(1), 25−29.
35 Sun, H.; Han, J. X.; Ding, Y. Q.; Li, W.; Duan, J. Z.; Chen, P.; Lou, H.; Zheng, X. M. One-pot synthesized mesoporous Ca/SBA-15 solid base for transesterification of sunflower oil with methanol. Appl. Catal. A-Gen. 2010, 390(1-2), 26−34.
36 Nair, P. A.; Ramesh, P. Synthesis and characterization of poly(urethane-ether)s from calcium salt of *p*-hydroxybenzoic acid. J. Appl. Polym. Sci. 2011, 122(3), 1946−1952.
37 Wang, Z. Q.; Yang, X. G.; Li, J. G.; Liu, S. Y.; Wang, G. Y. Synthesis of high-molecular-weight aliphatic polycarbonates from diphenyl carbonate and aliphatic diols by solid base. J. Mol. Catal. A-Chem. 2016, 424, 77−84.
38 Zhu, W. X.; Huang, X.; Li, C. C.; Xiao, Y. N.; Zhang, D.; Guan, G. H. High-molecular-weight aliphatic polycarbonates by melt polycondensation of dimethyl carbonate and aliphatic diols: synthesis and characterization. Polym. Int. 2011, 60(7), 1060−1067.
39 Liu, F.; Yang, X. G.; Li, J. G.; Liu, S. Y.; Yao, J.; Chen, T.; Wang, G. Y. Synthesis of poly (butylene carbonate) by melt transesterification of diphenyl carbonate and 1,4-butanediol. Acta Polymerica Sinica (in Chinese) 2014, (5), 628−635.
40 Naik, P. U.; Refes, K.; Sadaka, F.; Brachais, C. H.; Boni, G.; Couvercelle, J. P.; Picquet, M.; Plasseraud, L. Organo-catalyzed synthesis of aliphatic polycarbonates in solvent-free conditions. Polym. Chem. 2012, 3(6), 1475−1480.
41 Wang, Z. Q.; Bai, Y. S.; Jiang, W.; Yang, X. G.; Liu, S. Y.; Wang, G. Y. Structure-activity correlations of calcined Mg-Al hydrocalcites for aliphatic polycarbonate synthesis *via* transesterification process. Chinese J. Polym. Sci. 2017, 35(1), 130−140.
42 Wang, Z. Q.; Yang, X. G.; Li, S. Y.; Hu, J.; Zhang, H.; Wang, G. Y. One-pot synthesis of high-molecular-weight aliphatic polycarbonates via melt transesterification of diphenyl carbonate and diols using $Zn(OAc)_2$ as a catalyst. RSC Adv. 2015, 5(106), 87311−89319.
43 Kresge, C. T.; Leonowicz, M. E.; Roth, W. J.; Vartuli, J. C.; Beck, J. S. Ordered mesoporous molecular sieves synthesized by a liquid-crystal template mechanism. Nature 1992, 359(6397), 710−712.
44 Radwan, N. R. E. Influence of La_2O_3 and ZrO_2 as promoters on surface and catalytic properties of CuO/MgO system prepared by sol-gel method. Appl. Catal. A-Gen. 2006, 299(17), 103−121.
45 Tian, B. Z.; Liu, X. Y.; Yu, C. Z.; Gao, F.; Luo, Q; Xie, S. H.; Tu, B.; Zhao, D. Y. Microwave assisted template removal of siliceous porous materials. Chem. Commun. 2002, 11, 1186−1187.
46 Jiang, Q.; Wu, Z. Y.; Wang, Y. M.; Cao, Y.; Zhou, C. F.; Zhu, J. H. Fabrication of photoluminescent ZnO/SBA-15 through directly dispersing zinc nitrate into the as-prepared mesoporous silica occluded with template. J. Mater. Chem. 2006, 16(16), 1536−1542.
47 Di Cosimo, J. I.; Díez, V. K.; Xu, M.; Iglesia, E.; Apesteguía, C. R. Structure and surface and catalytic properties of Mg-Al basic oxide. J. Catal. 1998, 178(2), 499−510.
48 Zheng, L. P.; Xia, S. X.; Hou, Z. T.; Zhang, M. Y.; Hou, Z. Y. Transesterification of glycerol with dimethyl carbonate over Mg-Al hydrotalcites. Chin. J. Catal. 2014, 35(3), 310−318.
49 Hájek, M.; Kutálek, P.; Smolákováet, L.; Troppová, I.; Čapek, L.; Kubička, D.; Kocík, J.; Thanh, D. N. Transesterification of rapeseed oil by Mg-Al mixed oxides with various Mg/Al molar ratio. Chem. Eng. J. 2015, 263, 160−167.

https://doi.org/10.1007/s10118-018-2137-4